Stem Cell Reports
Article

OPEN ACCESS

Differentiation of Human Induced Pluripotent or Embryonic Stem Cells Decreases the DNA Damage Repair by Homologous Recombination

Kalpana Mujoo,[1,2,*] Raj K. Pandita,[1] Anjana Tiwari,[1] Vijay Charaka,[1] Sharmistha Chakraborty,[1] Dharmendra Kumar Singh,[1] Shashank Hambarde,[1] Walter N. Hittelman,[3] Nobuo Horikoshi,[1] Clayton R. Hunt,[1] Kum Kum Khanna,[4] Alexander Y. Kots,[5] E. Brian Butler,[1] Ferid Murad,[5] and Tej K. Pandita[1,6,*]

[1]Department of Radiation Oncology, Weill Cornell Medical College, The Houston Methodist Hospital Research Institute, Houston, TX 77030, USA
[2]Institute of Molecular Medicine, University of Texas Health at Houston, Houston, TX 77030, USA
[3]Department of Experimental Therapeutics, University of Texas MD Anderson Cancer Center, Houston, TX 77030, USA
[4]QIMR Berghofer Medical Research Institute, Brisbane, QLD 4029, Australia
[5]The George Washington University, Washington, DC 20037, USA
[6]Lead Contact
*Correspondence: kmujoo@houstonmethodist.org (K.M.), tpandita@houstonmethodist.org (T.K.P.)
https://doi.org/10.1016/j.stemcr.2017.10.002

SUMMARY

The nitric oxide (NO)-cyclic GMP pathway contributes to human stem cell differentiation, but NO free radical production can also damage DNA, necessitating a robust DNA damage response (DDR) to ensure cell survival. How the DDR is affected by differentiation is unclear. Differentiation of stem cells, either inducible pluripotent or embryonic derived, increased residual DNA damage as determined by γ-H2AX and 53BP1 foci, with increased S-phase-specific chromosomal aberration after exposure to DNA-damaging agents, suggesting reduced homologous recombination (HR) repair as supported by the observation of decreased HR-related repair factor foci formation (RAD51 and BRCA1). Differentiated cells also had relatively increased fork stalling and R-loop formation after DNA replication stress. Treatment with NO donor (NOC-18), which causes stem cell differentiation has no effect on double-strand break (DSB) repair by non-homologous end-joining but reduced DSB repair by HR. Present studies suggest that DNA repair by HR is impaired in differentiated cells.

INTRODUCTION

Stem cells have the dual ability to self-renew over the lifetime of an organism and also to differentiate into multiple cell lineages (Weissman et al., 2001; Seita and Weissman, 2010). The majority of mammalian cells *in situ* originate from a corresponding progenitor daughter cell that is terminally differentiated. Various factors, including reactive oxygen species, that accumulate during differentiation and over the stem cell lifespan, can cause DNA damage (Mikhed et al., 2015). In addition, differentiation-dependent changes in chromatin structure and transcriptional alterations (Nashun et al., 2015; Tran et al., 2015) can also affect genomic integrity by altering the DNA damage response (DDR) and repair facility. Thus, genomic stability is likely to be under increased stress during differentiation. How factors that induce differentiation, such as NO donors, affect stem cell genomic stability is unclear.

Stem cells benefit throughout their lifetime from a robust DNA damage repair activity that enhances resilience toward various environmental factors. Indeed, somatic cells and stem cells differ significantly in their radio-sensitivity (Chlon et al., 2016; Maynard et al., 2008; Lan et al., 2012; Momcilovic et al., 2009; Wilson et al., 2010). However, it is not known how DNA double-strand break (DSB) repair mechanisms are affected during stem cell differentiation. In order to understand whether stem cell differentiation affects DNA damage repair, we compared DDRs and DNA repair in human embryonic stem cells (ESCs) and induced pluripotent stem cells (iPSCs) with their isogenic, differentiated progeny, including neural progenitor cells (neuroectodermal lineage) and their subsequent differentiation products: astrocytes and dopaminergic neurons. DNA damage repair by homologous recombination (HR) was significantly reduced after cell differentiation in all cells examined.

RESULTS

Characterization of Differentiation Markers in iPSCs

Human iPSCs (B12-2) and ESCs (H-9) were used to compare the DDR between undifferentiated and differentiated cell status. The cell lines used were positive for OCT4 or Nanog (Figure 1A) and cell markers (ectoderm β-III tubulin [TUJ1], mesoderm smooth muscle actin [SMA], and endoderm alpha-feto protein [AFP]) and confirmed for embryoid body (EB)-directed differentiation into the three germ layers. During EB-directed differentiation, the first germ layer to be formed is ectoderm, which is identified by the cell marker (TUJ1) in our temporal differentiation (d11). Further, from d14 onward, all three germ layers were observed as indicated (Figure 1B). In other words, on day 11 only TUJ1 stained well; SMA and AFP did not stain,

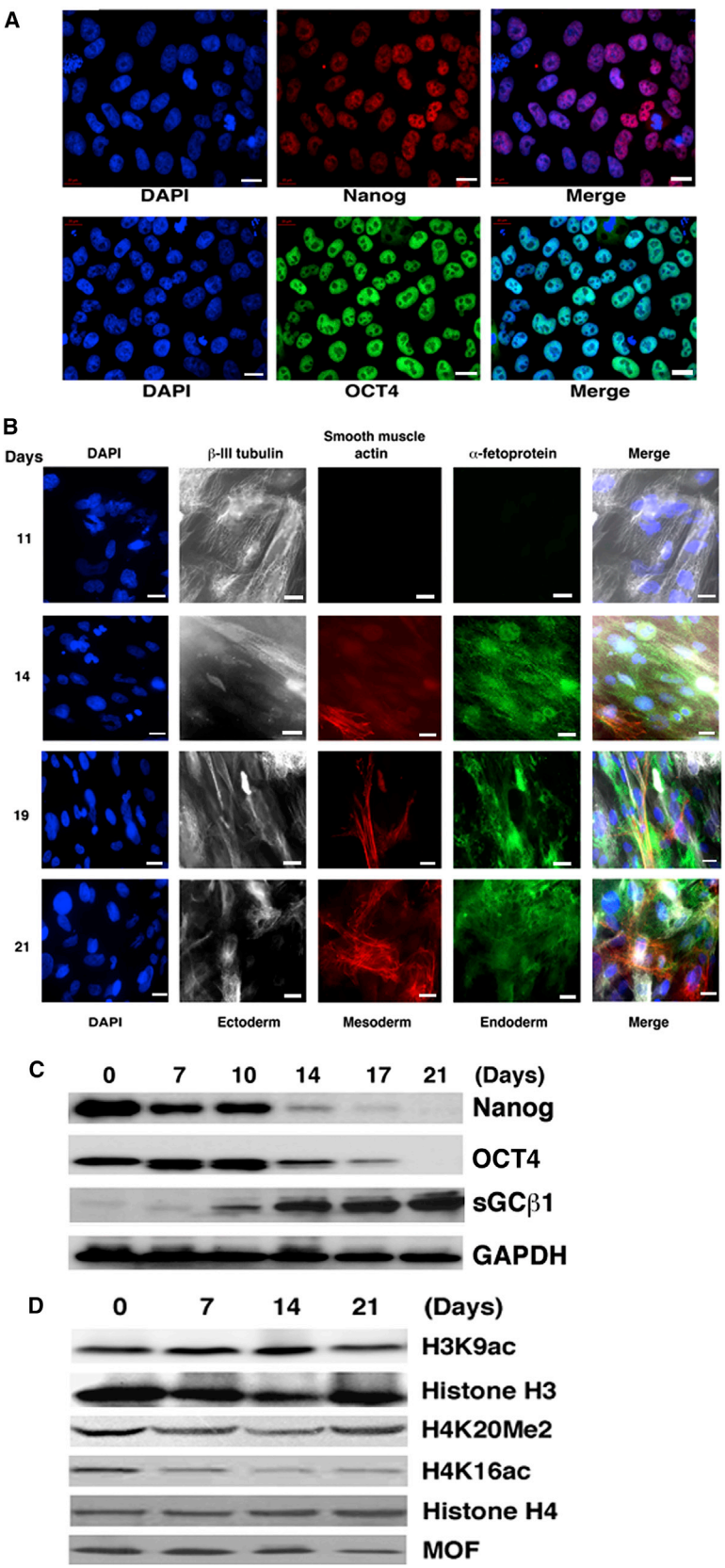

Figure 1. Differentiation-Induced Changes in Stem Cell Markers and Histone Modifications

(A) Immunostaining with antibody against Nanog and OCT4 in iPSCs. Scale bar, 10 μm.

(B) Immunostaining with different antibodies to detect stem cell differentiation into three germ layers. Scale bar, 10 μm.

(C and D) Western blot showing Nanog and OCT 4 and sGC β1 levels during various stages of differentiation (C) and western blot showing MOF, Histone H4, H4K16ac H3K9ac, Histone H3, and H4K20Me2 levels during temporal differentiation (D). Each experiment was done three independent times.

which is reflected in the Figure 1B. Western blot analysis revealed a time-dependent decrease in Nanog, OCT4 (Figure 1C), and hMOF (Figure 1D), while sGCβ1 (Figure 1C) protein levels increased during differentiation. Levels of the hMOF acetylation product H4K16ac were also reduced in differentiated cells (Figure 1D) (Gupta et al., 2008; Kumar et al., 2011; Thomas et al., 2008; Li et al., 2012). During differentiation, levels of H4K20me2 and H3K9ac were not significantly reduced (Figure 1D).

NO Donors Induce Genomic Instability in Stem Cells

We examined whether NO donors induced differentiation by treating stem cells with NOC-18 (5 μM). Differentiation markers such as NKx2.5 (Figure 2A) and myosin light chain 2 (MLC2) protein (Figure 2B) were found to be significantly increased compared with controls. These results are consistent with our earlier report (Mujoo et al., 2008). To determine whether NO also induces DDR, differentiated cells were treated with NOC-18 (0.5 mM) at a sub-toxic dose (95% survival), and response markers were analyzed by western blot and for signaling/repair factor foci formation. Phosphorylation of ATM as well as that of Chk1, Chk2, and H2AX (Figure 2C) was detected in western blots, all indications of DDR activation by NO. Treatment of stem and differentiated cells with NO also resulted in a significant increase in γ-H2AX, 53BP1, and RAD51 foci formation (Figures 2D–2F, S1A, and S1B). There was no difference in the levels of DNA DSB damage induced by ionizing radiation between stem and differentiated cells, indicating that susceptibility to initial damage is independent of differentiation status (Figure S1C). Overall, these results are consistent with previous reports observed in various primary and cancer cells (Fionda et al., 2015; Nagane et al., 2015; Oleson et al., 2014).

DNA DSB and Chromosome Aberration Analysis in Undifferentiated and Differentiated Cells

We next examined DSB rejoining of IR-induced DSBs by the Comet assay and found a significant increase in residual/unrepaired DSBs in differentiated cells compared with undifferentiated cells (Figures 3A and 3B), suggesting that differentiated cells have a reduced DSB repair capacity. The increased residual DSBs observed in differentiated cells correlated with chromosome aberrations when measured by basal level and IR-induced chromosome aberrations at metaphase. Differentiated cells were found to have a significantly higher frequency of chromosome aberrations (breaks, gaps, radials, dicentrics, micronuclei, aneuploids, and polyploids) compared with undifferentiated cell (Figures 3C and S2A–S2C). About 8%–12% of differentiated cells had chromatin blebbing (Figures 3D and S2D), with a high frequency of micronuclei and endo-reduplicated chromosomes (Figure S2D). Analysis of the cell-cycle specificity of the IR-induced chromosome aberrations indicated no significant differences between undifferentiated and differentiated cells in IR-induced G1-specific aberrations (Figure 3Ei), suggesting that the non-homologous end-joining (NHEJ) repair pathway is largely intact. However, the frequency of S-phase-specific chromosome aberrations was significantly higher in differentiated cells compared with undifferentiated cells (Figure 3Eii), while G2-type chromosomal aberrations did not show any significant differences (Figure 3Eiii). The differentiated cells did not have a significantly decreased percentage of S-phase cells, as there was no significant difference in 5-ethynyl-2′-deoxyuridine labeling between undifferentiated and differentiated cells (Figures S3A and S3B). Since DSB repair by HR occurs largely in S phase, the present data suggest that differentiated cells may have defects in the HR repair pathway.

DDR in Undifferentiated Stem Cells and Differentiated Cells

The initial events of DDR are ATM autophosphorylation and H2AX phosphorylation at Ser139 (γ-H2AX). The frequency of IR-induced γ-H2AX foci induction, which can serve as a surrogate marker for DNA DSBs, was initially identical in undifferentiated and differentiated cells. However, γ-H2AX foci disappearance was delayed in differentiated cells, indicating compromised DSB repair (Figures 4A and S3C). The induction of IR-induced γ-H2AX foci was identical in differentiated ESCs (Figures S4A and S4B) and iPSCs (Figure 4A), suggesting the overall sensing of DNA damage is not affected by differentiation. The higher frequency of residual γ-H2AX foci in differentiated cells indicates a defect in DSB repair that could lie in either the NHEJ and/or HR pathway, although the chromosome aberration data above suggest HR is most likely compromised.

Repairosome Foci Analysis of HR-Related Protein Factors

The 53BP1 protein is involved in suppression of HR (Morales et al., 2003; Ward et al., 2003; Zimmermann et al., 2013), and the first downstream effector of 53BP1 activity is RIF1 (Chapman et al., 2013; Di Virgilio et al., 2013; Escribano-Diaz and Durocher, 2013; Escribano-Diaz et al., 2013; Feng et al., 2013; Zimmermann et al., 2013). While the initial formation of 53BP1 foci post irradiation was identical; there was a significant delay in 53BP1 foci clearance in differentiated cells (Figure 4B). The frequency of RIF1/53BP1 foci co-localization was also higher in differentiated cells compared with undifferentiated cells (Figures 4C–4E). Accumulation of RIF1 at DSB sites containing phosphorylated 53BP1 (Anbalagan et al., 2011; Bonetti et al., 2010) inhibits the DNA resection step of HR (Bunting et al., 2010), suggesting differentiation-dependent suppression

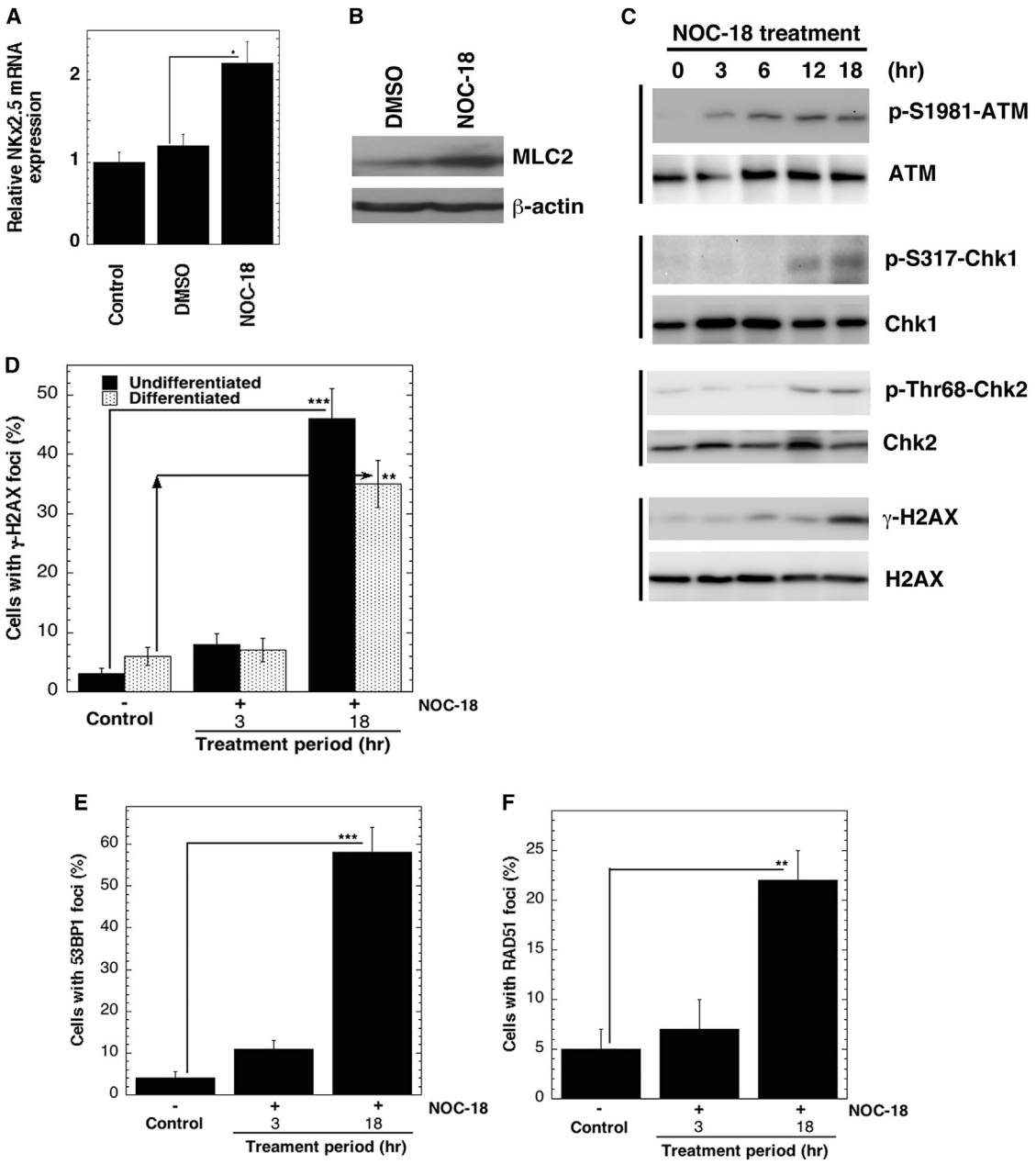

Figure 2. Nitric Oxide Induced Stem Cell Differentiation and DNA Damage Response

(A) Partially differentiated cells (d7 EBs) were exposed to the NO donor NOC-18 (5 μM) on days 7, 9, 11, and 13, and the cells were harvested on day 14 for RNA sample analysis by real-time qPCR for NKx2.5. Error bars indicate ±SEM. Significance using paired Student's t test is shown. *$p < 0.05$; n = 4–7, repeated thrice independently.

(B) Cellular proteins extracted from differentiated cells exposed to NO donor analyzed for MLC2 and β-actin by western blotting.

(C) Differentiated cells treated with sub-toxic concentrations (0.5 mM) of NO donor (NOC-18) and examined for activation of ATM, Chk1, Chk2, and γ-H2AX by western blotting.

(D–F) Differentiated cells exposed to 0.5 mM NO donor (NOC-18) for 18 hr then immunostained and analyzed for γ-H2AX (D), 53BP1 (E), and RAD51 (F) foci formation. Each experiment was performed three to four times independently, and for each time point, a minimum of 200 cells was scored. **$p < 0.01$; ***$p < 0.001$.

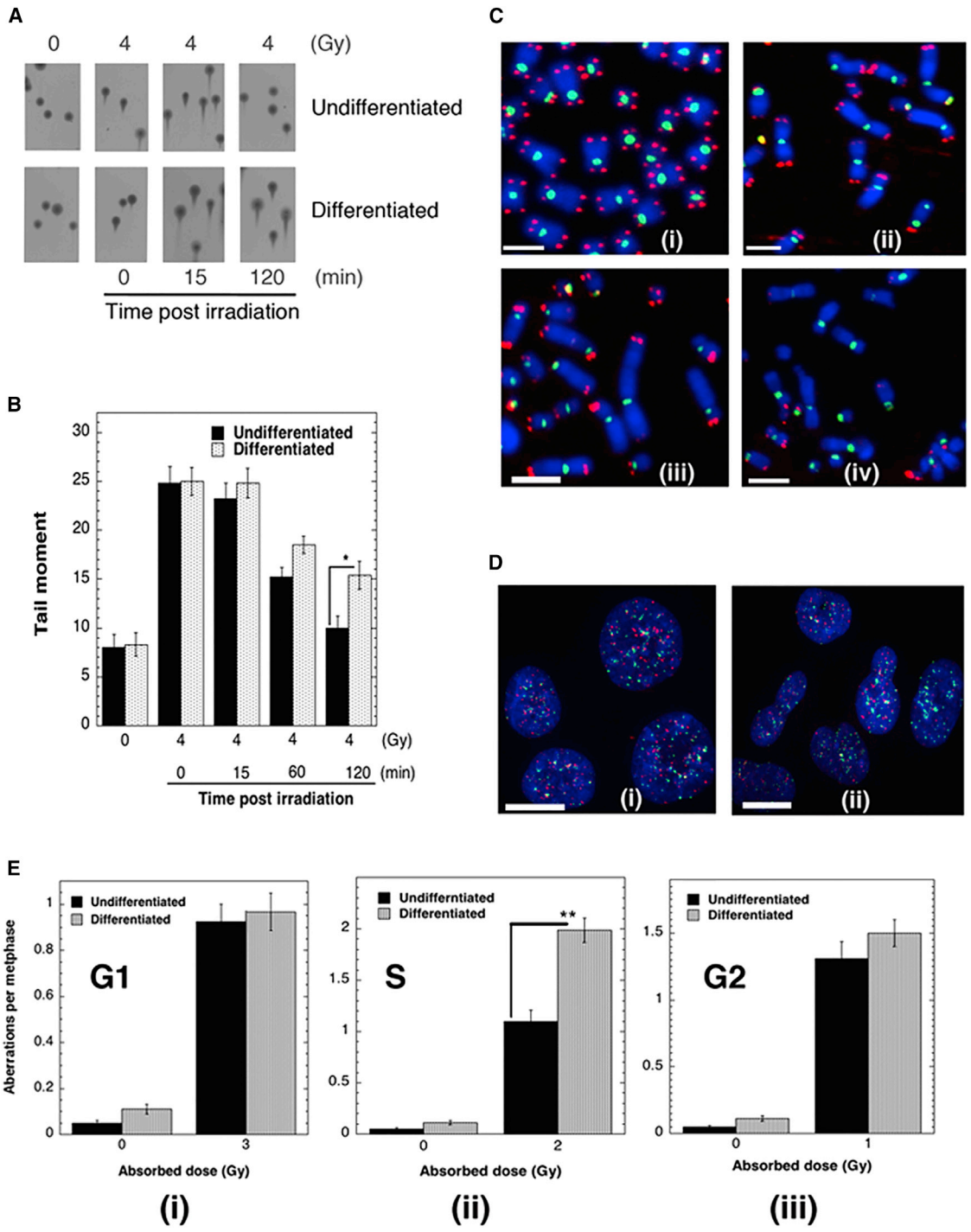

Figure 3. Measurement of Chromosome Aberrations and DNA Damage in Stem Cells and Differentiated Cells

(A) DSBs in stem and differentiated cells after exposure to 4 Gy were detected by neutral Comet assay at intervals up to 120 min.

(B) Quantitative analysis of mean tail moment (time course) in stem cells and differentiated cells post exposure to IR. The results are from four independent experiments. Error bars indicate ±SEM. Significance using paired Student's t test is shown. *$p < 0.05$.

(C) Metaphase chromosomes-telomere FISH (i) undifferentiated stem cells; (ii) differentiated cells showing loss of telomeres and dicentric-type chromosome aberrations; (iii) fusion of chromosomes and dicentric; (iv) loss of telomeres and centromeres.

(D) Micronuclei and chromosome blebbing: (i) undifferentiated cells; (ii) differentiated cells.

(legend continued on next page)

of HR-mediated DSB repair. Cellular levels of RAD51 and Chk2 proteins are similar in differentiated versus undifferentiated cells but Chk2 phosphorylation at Thr68 increases during differentiation (Figures 4Fi, 4Fii, and 4Fiii).

Formation of MDC1 repairosomes was identical between undifferentiated and differentiated cells (Figure 5A), but a significant decrease in BRCA1 and RAD51 foci formation after irradiation was observed in differentiated cells (Figures 5B, 5C, and S4C). The reduced frequency of IR-induced BRCA1 and RAD51 foci could affect DNA resection, an early step in HR-mediated repair, and when we examined resection-related proteins for repairosome formation, lower levels of IR-induced MRE11, RAP80, and FANCD2 foci were detected in differentiated cells (Figures 5D–5F). The data supports the argument that differentiated stem cells have a reduced ability to repair DSBs by HR, probably due to failure to displace 53BP1 and allow subsequent HR proteins to load at the DSB site.

We further examined whether the DDR is similarly altered when primitive cells derived from a developing animal organ are fully differentiated *in vitro*. Later-stage astrocytes had a higher frequency of cells with delayed disappearance of γ-H2AX foci and a reduced number of RAD51 foci, indicating that differentiated astrocytes showed a similar DDR defect as observed in the stem cell-derived differentiated cells (Figures S5A–S5E), suggesting decreased HR is a general feature of cell differentiation.

In addition to repair of IR-induced DNA damage, HR-mediated repair is applicable to other types of damage, especially that arising from replication fork blockage and stalling (Gupta et al., 2014b; Hunt et al., 2013). Interstand cross-links (ICLs) create obstructions to fundamental DNA processes and are repaired predominantly during S phase when replication forks converge at ICL sites (Raschle et al., 2008). We first examined the repair of DNA damage induced by camptothecin, which binds to topoisomerase 1 and forms a DNA covalent complex that is specifically repaired by HR. After camptothecin treatment, differentiated cells exhibited delayed loss of γ-H2AX foci and a lower frequency of RAP80 foci compared with undifferentiated cells (Figures 5G and 5H). Similarly, treatment with the DNA cross-linking drug cisplatin induced a higher frequency of cells with delayed disappearance of γ-H2AX foci in differentiated cells (Figure 5I). Furthermore, RAD51 foci formation, a marker of HR, after cisplatin or hydroxyurea (HU) treatment was reduced in differentiated cells (Figures 5J and 5K).

DDR in Neural Progenitor Cells and Differentiated Astrocytes or Dopaminergic Neurons

Neural progenitor cells (NProC), prepared from B12-2 iPSCs, are of neuro-ectodermal origin and PAX 6 positive/OCT4 negative (PAX 6+/OCT4–) (Figure S6A). Following NProC cell differentiation, mature astrocytes were detected as glial fibrillary acidic protein (GFAP) positive (Figure S6B) and mature dopaminergic neurons as β III tubulin (TUJ1) positive (Figure S6C). iPSCs (B12-2), progenitors (NOProC), and differentiated cells were exposed to IR and foci formation by the HR markers (RAD51 and BRCA1), NHEJ (53BP1 and RIF1), and γH2AX were measured (Figure 6). There was a significant delay in the disappearance of γ-H2AX foci in neural progenitors, astrocytes, and dopaminergic neurons (Figure 6A) and an associated delay in 53BP1 and RIF1 foci clearance compared with undifferentiated cells (Figures 6B and 6C). These results are consistent with mixed-culture differentiated cells (Figures 3 and 4). Moreover, BRCA1 and RAD51 foci were correspondingly reduced in astrocytes and dopaminergic neurons compared with neural progenitor cells (Figures 6D and 6F). Figure 6E is a representative photomicrograph of DAPI (a) 53BP1 (b), and RAD51 foci (c) in astrocytes. These results provide further support for the model that HR-mediated DDR is significantly downregulated in terminally differentiated cells such as astrocytes and dopaminergic neurons.

Impact of Differentiation on DNA Replication Fork Stalling and Resolution

To determine whether reduced RAD51 and BRCA1 foci formation after treatment with agents that induce interstrand cross-links in differentiated cells is due to altered restart of stalled replication forks, we measured the frequency of stalled replication forks and new replication origin firing by using the chromatin fiber assay (Henry-Mowatt et al., 2003). Cells were pulse-labeled with 5-chlorodeoxyuridine (CldU) followed by HU treatment for 2 hr to deplete the nucleotide pool, and subsequently labeled with 5-iododeoxyuridine (IdU) (Petermann et al., 2010; Singh et al., 2013). Contiguous IdU/CldU signals (Figures 7A and 7B),

(E) Analysis of cell-cycle-specific residual chromosome damage in undifferentiated and differentiated cells with chromosomal aberration analyzed at metaphase; G1 (i), S (ii), and G2 (iii) cell-cycle phase aberrations include dicentrics, centric rings, interstitial deletions/acentric rings, and terminal deletions; all categories of asymmetric chromosome aberrations were scored; differentiated cells showed significantly higher chromosomal aberration frequencies compared with control cells (**$p > 0.01$, Student's t test, $n = 3$). Each experiment was done thrice, and for each time point, 150 metaphases were scored for chromosomal aberrations and 225 metaphases were analyzed for telomere signals.
Scale bar, 10 μm.

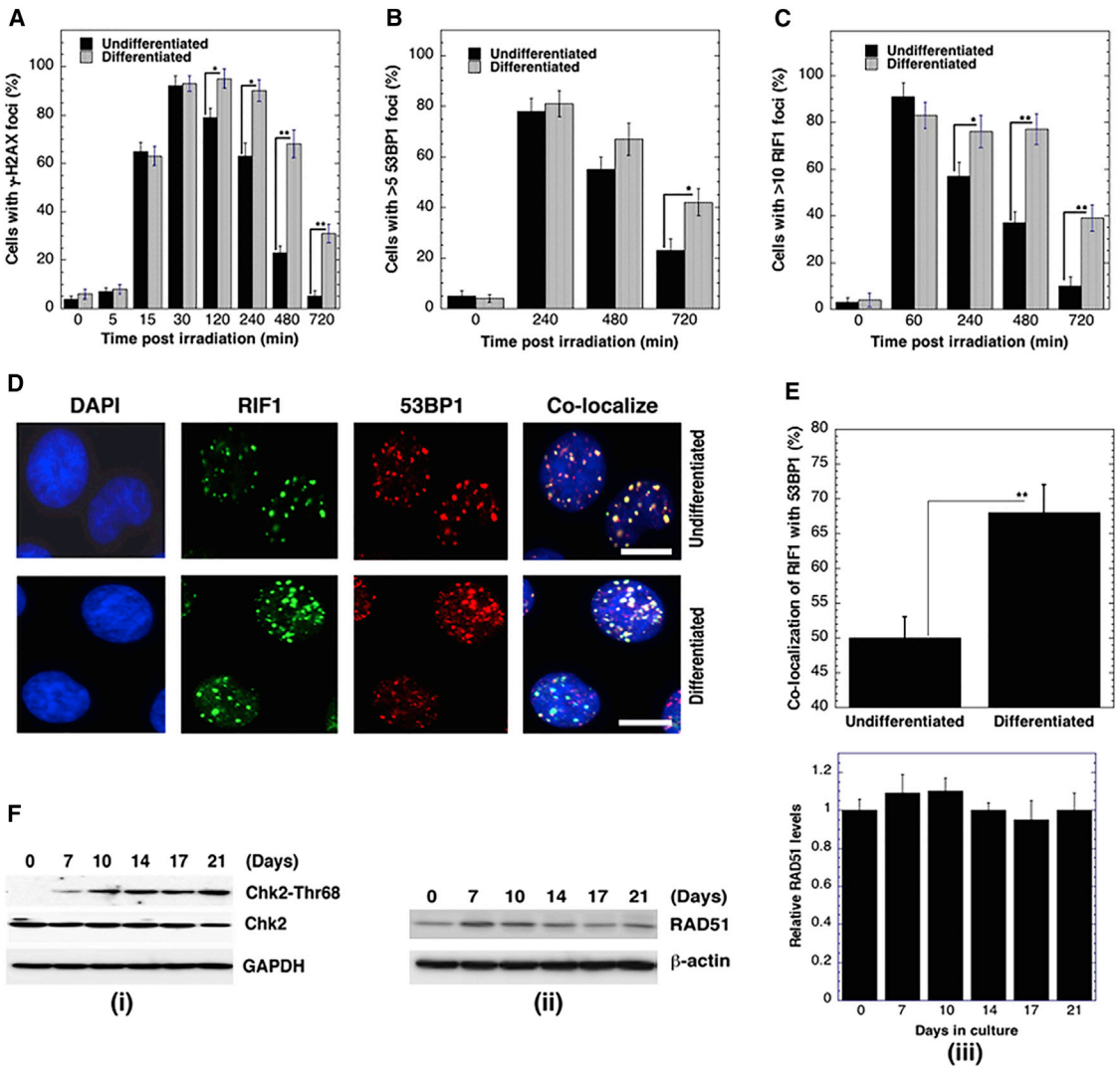

Figure 4. DNA Damage Response in iPSCs and Differentiated Cells

(A–C) B12-2 and differentiated cells were exposed to IR (A), γ-H2AX (2 Gy), (B) 53BP1 (6 Gy), and (C) RIF1 (6 Gy), then stained and analyzed for foci formation. Error bars indicate ±SEM. Significance using paired Student's t test is shown. *p < 0.05, **p < 0.01, n=3.

(D) Co-localization of 53BP1 and RIF in B12-2 and differentiated cells.

(E and F) Quantitation of RIF1 and 53BP1 co-localization; **p < 0.01, n=3 (E); 53BP1 and RIF1 foci were counted for 3 sets of 25 cells and the percentage of co-localized 53BP1/RIF1 foci calculated relative to total number of foci (53BP1+RIF1); western blotting of Chk2 (Fi), RAD 51 (Fii), and histogram showing relative levels of RAD51 (mean of three blots) (Fiii) during differentiation of iPSCs. For foci scoring, 600 cells from three independent experiments for each time point were scored.

Scale bar, 10 μm.

identifying restarted forks, were significantly lower in differentiated than in undifferentiated iPSCs (B12-2) or ESCs (H9) (Figures 7Ci and 7Di). Further analysis of the DNA fibers indicated the percentage of stalled forks in differentiated cells after 2 hr of HU treatment was higher than in undifferentiated cells, suggesting that differentiated cells resolve stalled replication forks less efficiently in both iPSCs (B12-2) and ESCs (H9) (Figures 7Cii and 7Dii). In addition, differentiated cells had a shorter DNA tract length distribution, indicating reduced replication fork speeds (Figures 7E and 7F).

Replication fork stalling can also arise from RNA:DNA hybrid formation, the latter also referred to as transcriptional R loops. We observed a higher frequency of R-loop formation in differentiated than in undifferentiated cells (Figures S7A and S7B).

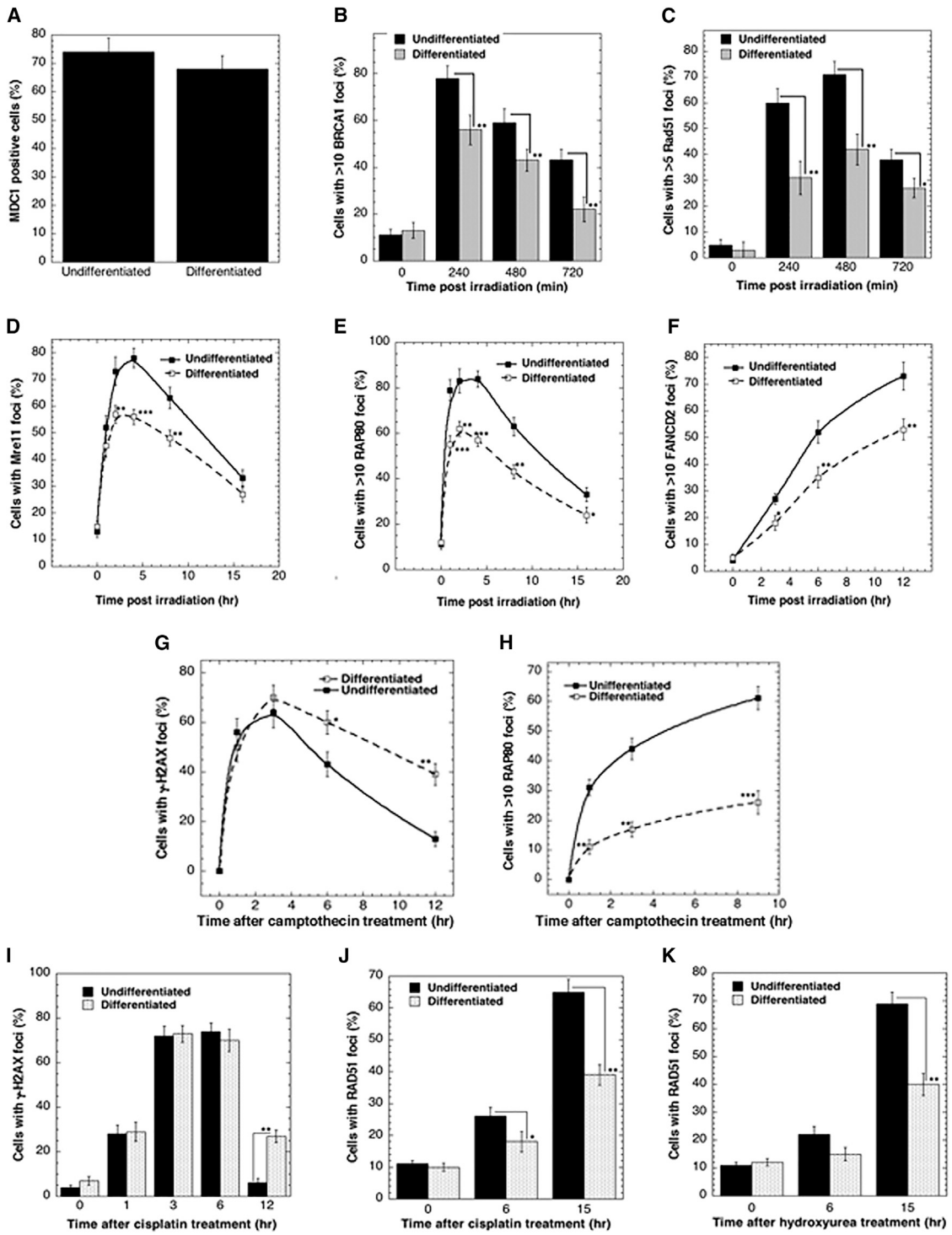

Figure 5. HR Repair Factor Foci Formation after DNA Damage in Undifferentiated and Differentiated Cells

Stem cells and differentiated cells were exposed to various doses of IR and immunostained with the respective antibodies to measure the percentage of immune-positive cells with MDC1 foci (A), with BRCA1 foci (B), Rad51 foci (C), Mre11 foci (D), RPA 80 (E), and FANCD2 (F). Images were captured using a Zeiss Axio Scope fluorescent microscope and foci scored with ImageJ software (v1.47, NIH). B12-2 and

(legend continued on next page)

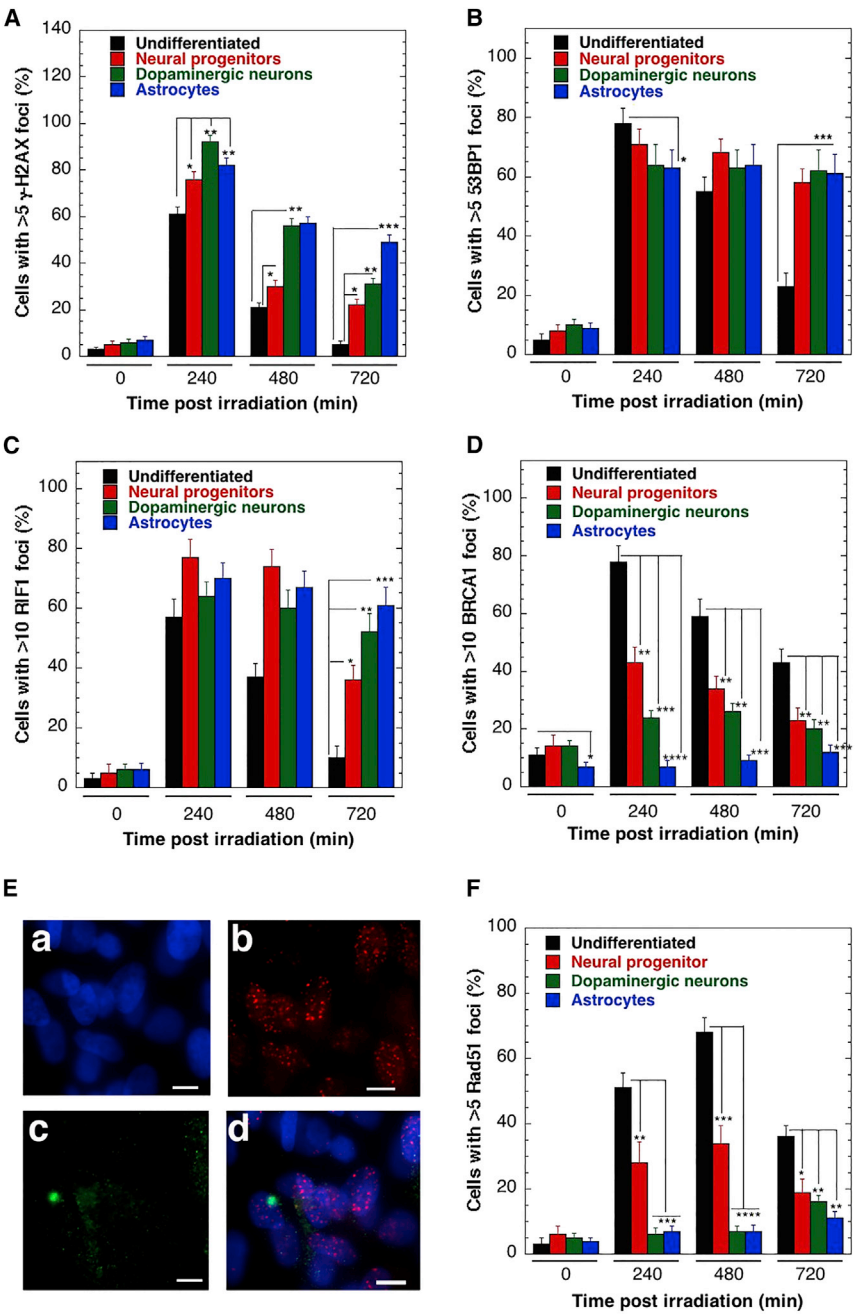

Figure 6. DNA Damage Response in Neural Progenitor Cells, Astrocytes, and Dopaminergic Neurons

(A–D and F) The cells (undifferentiated, neural progenitors, astrocytes, and dopaminergic neurons) were exposed to various doses of IR (A), γ-H2AX (2 Gy), (B) 53BP1 (6 Gy), (C) RIF1 (6 Gy), (D) BRACA1 (10 Gy), and RAD51 (F) then stained and analyzed for foci formation.

(E) Representative photograph showing RAD51 foci in comparison with 53BP1 foci formation in astrocytes. Significance using paired Student's t test is shown. *p < 0.05; **p < 0.01, ***p < 0.001, ****p < 0.0001, n = 3. For foci scoring, 600 cells from three independent experiments for each time point were scored.

Scale bar, 10 μm.

Finally, we directly tested whether NO could affect DSB repair by NHEJ or HR or both pathways by using GFP gene reconstitution assays (Pandita et al., 2006; Pierce et al., 1999). Stably transfected cell lines containing the appropriate GFP substrate constructs were transiently transfected with an I-SceI expression vector and simultaneously treated with a sub-toxic dose of the NO donor NOC-18 (0.5 mM; 5% toxicity). Fluorescent GFP-positive cells, indicating repair of the I-Sce1-induced DSB, were detected by fluorescence-activated cell sorting (FACS)

differentiated cells were exposed to campathecin (100 nM), cisplatin (2 μM), or hydroxyurea (2 mM) to induce DNA damage and campathecin-induced γ-H2AX (G) and RPA80 (H), cisplatin-induced γ-H2AX (I) and Rad51 (J), and hydroxyurea-induced Rad51 (K) foci were measured after staining with the respective antibodies. Significance using paired Student's t test is shown. *p < 0.05; **p < 0.01, ***p < 0.001, n = 3. For foci scoring, 600 cells from three independent experiments for each time point were scored.

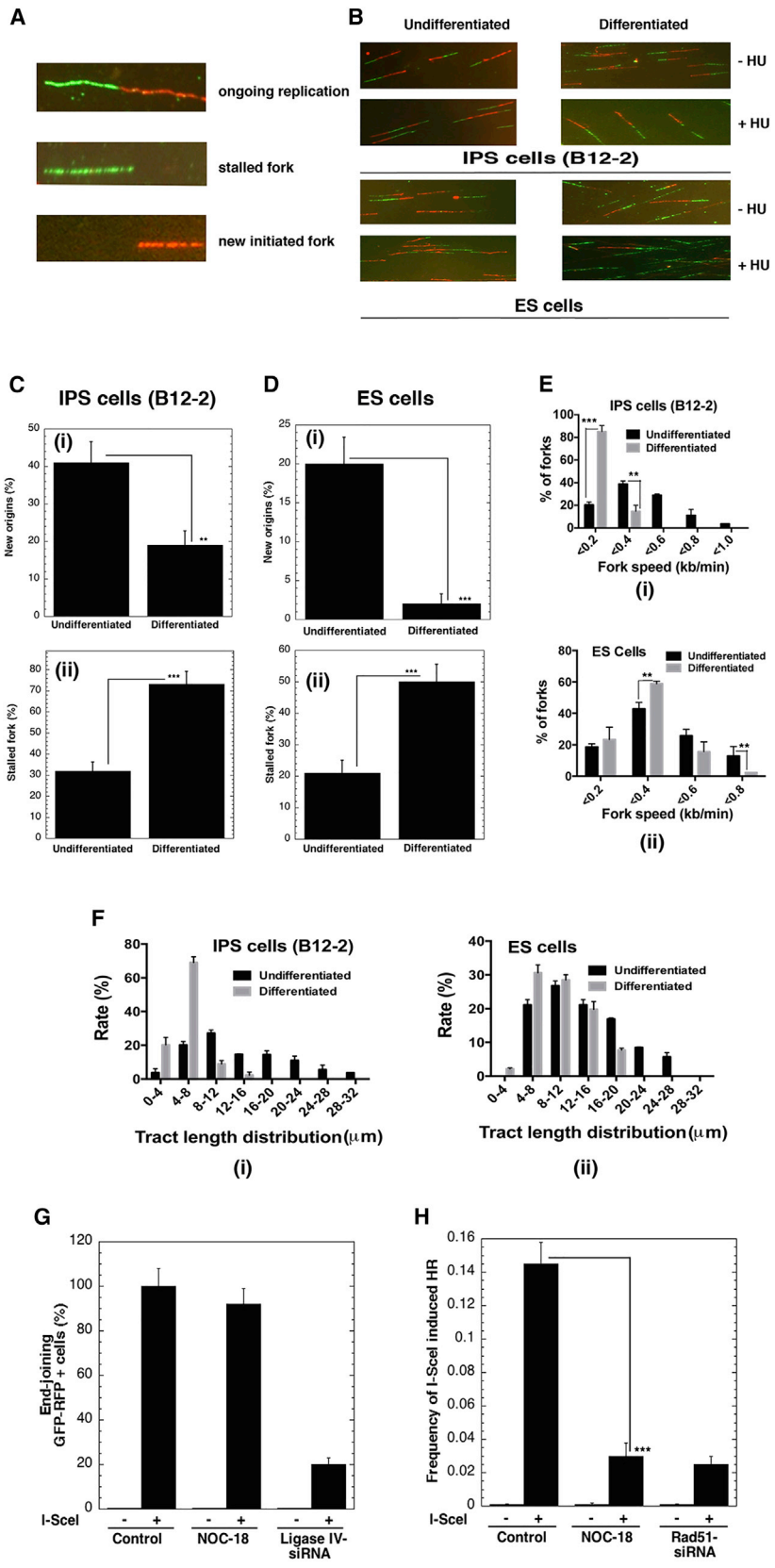

Figure 7. Stalled DNA Replication Forks and Initiation of New Origins in B12-2 and Differentiated Cells

(A and B) DNA labeling and hydroxyurea treatment protocol for single DNA fiber analysis showing ongoing replication (green IdU followed by red CldU track; green only tracks indicate stalled forks and red only tracks identify newly initiated replication sites) (A). Representative image of replication tracks from B12-2 (iPSCs) and H-9 ESCs and their differentiated progeny in the presence and absence of hydroxyurea, which depletes the nucleotide pool (B).

(C) Quantification of new origins as determined by CldU signal after 2 hr of HU treatment in B12-2 and differentiated cells and H-9 and differentiated cells. Significance by paired Student's t test is shown. $^{**}p < 0.01$, $^{***}p < 0.001$, n = 3.

(D) Differentiated cells show a decrease in incorporation of CldU and maximum frequency of cells with stalled forks. Significance by paired Student's t test is shown. $^{***}p < 0.001$, n = 3.

(E and F) Fork speed (E) and track length distribution (F) in undifferentiated (ESCs and iPSCs) and differentiated cells. Significance by paired Student's t test is shown. $^{**}p < 0.01$, $^{***}p < 0.001$, n = 3.

(G) Effect of NOC-18 on DSB repair as measured by NHEJ reporter assay.

(H) Effect of NOC-18 on DSB repair as measured by HR reporter assay. All experiments were done three to four independent times. $^{***}p < 0.001$, n = 3.

48 hr after transfection and the percentage of cells with repair was calculated. Treatment with the NO donor had no impact on DSB repair through the NHEJ pathway (Figure 7G) however; HR-mediated repair was significantly reduced, suggesting NO specifically affects DSB repair by the HR pathway (Figure 7H).

DISCUSSION

Continuing stem cell proliferation is necessary to generate cell populations of different lineages during development and for maintenance of tissue homeostasis. The critical role of stem cell expansion necessitates a high-fidelity-based mechanism to repair DNA damage since any mutations will compromise all the derived cell lineages (Adams et al., 2010; Serrano et al., 2011). Whether the high-fidelity-based DNA repair pathway that utilizes HR is maintained in differentiated progeny cells has been of great interest. We compared DSB repair in stem cells at undifferentiated and differentiated stages, and our previous studies have demonstrated that differentiation of stem cells is accompanied by NO production to activate the NO-cyclic GMP pathway (Mujoo et al., 2006, 2008; Mujoo et al., 2011). Moreover, modulation of NO levels post IR exposure can occur due to the conversion of oxidative species into nitrosative signals (Pacher et al., 2007; Pham-Huy et al., 2008; van Gent et al., 2001). We report that NO donors activate the ATM kinase pathway as well as induce DNA damage as detected by γ-H2AX and RAD51 foci formation, surrogate markers for DNA DSBs, in both undifferentiated and differentiated cells. When we compared the DDR in stem cells before and after differentiation, we found that differentiated stem cells have the following: (1) higher frequency of spontaneous chromosome aberrations; (2) reduced DNA DSB repair after IR exposure; (3) higher frequency of S-phase-specific IR-induced chromosome aberrations; (4) higher frequency of residual γ-H2AX foci formation after IR exposure or cisplatin treatment; (5) higher frequency of cells with 53BP1 and RIF1 co-localization; and (6) higher frequency of cells with a reduced number of RAD51 or BRCA1 foci after IR exposure or cisplatin treatment compared with undifferentiated stem cells. Furthermore, analysis of lineage-specific differentiation toward the neuronal pathway revealed that mature astrocytes and dopaminergic neurons have impaired DSB repair by HR compared with undifferentiated and neuronal progenitor cells. The higher frequency of chromosome aberrations found in differentiated cells correlated with reduced DSB repair and a higher frequency of S-phase-specific aberrations, suggesting that differentiation affects DSB repair. The higher frequency of chromosome aberrations is not due to an altered cell-cycle distribution as there is no difference in the distribution of cell-cycle phases between undifferentiated and differentiated cells. Since no difference in IR-induced G1- or G2-specific chromosome aberrations was observed between undifferentiated and differentiated cells, this suggests the NHEJ DSB repair pathway is not affected, as it is the dominant mode of DSB repair in G-1 or G-2 phase cells. In contrast, differentiated cells have a higher frequency of S-phase-specific IR-induced chromosome aberrations, suggesting that differentiation impairs HR DSB repair, which primarily occurs in S-phase cells. Thus, our results suggest that while the NHEJ pathway is minimally altered, DSB repair by HR is reduced by differentiation of stem cells.

Only a subset of differentiated cells had a higher frequency of residual IR-induced γ-H2AX foci, suggesting that most of the cells can repair the DNA damage. Further, since differentiated cells showed a higher frequency of cells with co-localization of 53BP1 with RIF1, this suggests that in such cells, the subsequent recruitment of the HR-related proteins is impaired. Consistent with these observations, differentiated cells have a reduced frequency of foci formation by RAD51, BRCA1, and other HR-related protein.

Defects in HR can also decrease resolution of stalled replication forks, and we found a higher frequency of stalled replication forks and lower frequency of new replication origins in differentiated stem cells. The increased level of stalled forks could be due to reduced resolution and repair of the forks by HR. Alternatively, increased interstrand cross-links or transcriptional RNA:DNA hybrids, also called R loops, may contribute to stalling. This latter mechanism seems more likely since differentiated cells exhibited a higher frequency of R loops. Further, the reduced levels of H4K16ac we found in differentiated cells may be important due to its unique ability to control chromatin structure and protein interactions, which may facilitate a more open, repair-conducive chromatin configuration (Pandita, 2013; Horikoshi et al., 2016). Acetylation of H4K16 also limits 53BP1 association with damaged chromatin to promote repair by the HR pathway (Tang et al., 2013). Thus, the reduced levels of H4K16ac in differentiated cells could be one of the factors contributing to aberrant DSB repair.

Mature astrocytes and dopaminergic neurons exhibit significantly higher residual damage, in comparison with their undifferentiated and neuronal progenitor cells, as demonstrated by the delayed disappearance of γ-H2AX foci 8–12 hr post irradiation. Similarly, compared with undifferentiated cells, delayed clearance of 53BP1 and RIF1 foci was observed in neural progenitors, mature astrocytes, and dopaminergic neurons, which is consistent with the correspondingly lower frequency of BRCA1 and RAD51 (HR proteins) foci formation in these cells. Our observations support previous studies indicating that both ESCs

and iPSCs repair DNA lesions by HR compared with their differentiated derivatives (Rocha et al., 2013). Some studies have also shown that, compared with neural stem cells, terminally differentiated descendant astrocytes lack functional DDR signaling. However, astrocytes retain the expression of NHEJ genes and are indeed DNA-repair proficient (Schneider et al., 2012). Future studies will focus on elucidating the molecular mechanisms of DNA DSB repair in stem cells and their lineage-directed progeny.

EXPERIMENTAL PROCEDURES

Reagents and Antibodies

Antibodies were from Cell Signaling: Chk1 (#2360), pChk1 (Ser317) (#12302S), Chk2 (#2662S), pChk2 (Thr68) (#2661), ATR (#2790S), pATM-Ser-1981 (#13050S), total H2AX (#7631), H2AX-Ser 139 (#9718), OCT 4 (#2890), nanog (# 4903) and GFAP (#3670s). Santa Cruz antibodies: 53BP1 (#sc-22760), ATM (#sc-7230), BRCA1 (#sc-642). Abcam antibodies: RPA-70 (#ab79398), Rad51 (#ab63801). Genetex antibodies: MRE11 (#GTX70212). Bethyl Laboratories antibodies: RIF1 (A300-5671). Upstate Biotechnology and Millipore: H2AX-Ser 139 (# 05-636), Molecular Probes (three germ layer kit) (#25,538).

Cell Culture and Differentiation of Human Induced Pluripotent Cells

Human iPSCs (clones B12–2 and B12-3) were a kind gift from Dr. Douglas Melton and Dr. D. Huangfu of the Harvard Stem Cell and Regenerative Center, MA. iPSCs (B12-2 or B12-3) were initially grown in 90% knockout DMEM, 10% knockout serum replacer, 10% Plasmanate (human plasma), 1 mM L-glutamine, 1 mM non-essential amino acids, 0.1 mM β-mercaptoethanol (55 mM Stock), supplemented with 10 ng/mL basic fibroblast growth factor on mitotically inactivated mouse embryonic fibroblast feeder layers. H-9 and B12-2 cells were also grown on Matrigel in mTeSR-1 medium (Stem Cell Technologies) for feeder-cell-free culture maintenance. For differentiation, H-9 cells and iPSCs grown on Matrigel were dissociated using 2 mg/mL collagenase IV (Invitrogen), washed and cultured in suspension in ultra-low attachment plates (Corning) in the differentiation medium containing 80% knockout DMEM, 1 mM L-glutamine, 0.1 mM β-mercaptoethanol, 1 mM non-essential amino acids, and 20% defined fetal bovine serum (Hyclone). The medium was changed on days 2 and 4, and on day 6 the EBs were transferred onto gelatin-coated plates (3–4 EBs per cm^2) and cultured for additional days as described in the Results section.

B12-2 (iPSCs) was generated by reprogramming primary human fibroblasts to pluripotent state (Huangfu et al., 2008). Cultures of undifferentiated ESCs or iPSCs were designated as day 0 control.

Treatment of Partially Differentiated Cells with NO Donors

To evaluate the effect of NO donor NOC-18 in differentiation of B12-2 cells, day 7 EBs were incubated with NO donors NOC-18 (5 μM). The agents were added to the cell culture on days 7, 9, 11, and 13 (multiple treatments). The cells were harvested between days 17 and 21, and marker genes and proteins were analyzed as indicated in the Results section.

Real-Time RT-PCR

Stem cell and derived differentiated cellular total RNA was isolated using TRIZOL reagent (Invitrogen, Carlsbad, CA). cDNA was prepared using a high-capacity cDNA archive kit (Applied Biosystems, Foster City, CA), according to the manufacturer's instructions. Real-time PCR assays for different subunits of sGC (α_1, β_1), Nkx2.5 and GAPDH were purchased from Applied Biosystems and determined using the manufacturer's suggested protocol. All reactions were conducted using a 7900 HT Prizm Sequence Detection System for 40 cycles. The results were analyzed using the $_2{}^{-\Delta\Delta C}{}_T$ method (Livak and Schmittgen, 2001).

Western Blot Analysis

Cell cultures washed with cold PBS were lysed in cell extraction buffer (Invitrogen) supplemented with 1 mM phenylmethyl sulfonyl fluoride and protease inhibitor cocktail (Sigma-Aldrich) for 30 min on ice. After fractionation by SDS-PAGE, the proteins were transferred to a nitrocellulose membrane and incubated with specific antibodies. Proteins were detected with horseradish peroxidase-conjugated secondary antibodies and visualized by enhanced chemiluminescence.

Detection of γ-H2AX Foci and Other DDR Components

Stem cells and differentiated cells in chamber slides (Nunc Lab-Tek II) were irradiated with 2–10 Gy (depending upon marker detection) then allowed to recover for 0.5–12 hr at 37°C. Following fixation and permeabilization, cells were probed with antibodies against phosphorylated H2AX-Ser136, RAD51, 53BP1, RIF1, BRCA1, MDC1, MRE11, FANCD2, and RAP 80. Foci formation by γ-H2AX and other proteins were visualized using a Zeiss Axio Scope fluorescent microscope and scored with the Image G software (v1.47, NIH). At least 100 cells were evaluated for each sample to ensure statistical reliability.

DNA Fiber Assay

DNA fiber spreads of ESCs (H-9); iPSCs (B12-2), and derived differentiated cells were prepared as described (Singh et al., 2013) with minor modifications. Briefly, ongoing replication sites in cells were labeled with IdU (50 μM) followed by exposure to HU (4 mM), washing, and labeling with CldU (50 μM). Fibers were quantified using ImageJ software.

Comet Assay

The neutral Comet assay measures DNA DSBs in single cells (Comet Assay Kit, Trevigen). Comet tail moments were measured in at least 100 cells and quantified using the CometScore software.

Chromosomal Aberration Analysis at Metaphase

Analysis was performed as described previously (Pandita et al., 2006) (Singh et al., 2013). Cells were irradiated with 3 Gy and analyzed for metaphase aberrations after 12 hr (Gupta et al.,

2014a). Cisplatin-induced chromosome aberrations were analyzed as described (Singh et al., 2013).

Non-homologous End-Joining and Homologous Recombination Reporter Assays

The NHEJ-specific assay was performed as previously described, with minor modifications (Gupta et al., 2014b; Udayakumar et al., 2016). The NHEJ reporter assay used an IRES_TK_EGFP reporter gene plasmid, a gift from T. Kohno (National Cancer Research Institute, Tokyo, Japan), and the assay was performed as previously described, with minor modifications (Ogiwara et al., 2011). The HR-specific assay used the DR-GFP cassette, and the HR reporter-based assay was performed as described with minor modifications (Pandita et al., 2006; Pierce et al., 1999). For both assays, the substrate constructs were stably transfected into H1299 cells, and an I-Sce1 expression construct was transiently co-transfected into cells pretreated with DMSO, NOC-18, or small interfering RNAs (siRNAs). The percentage GFP-positive cells was determined by FACS 48 hr after transfection. Depletion of Ligase IV for NHEJ and depletion Rad51 for HR by specific siRNA were used as positive controls for measuring NHEJ and HR efficiencies.

Neural Precursor Cell Derivation from B12-iPSCs

We used neural induction media (NIM) (Stem Cell Technologies) for generating neural precursor cells from monolayer culture of iPSCs as per the manufacturer's recommendations. Briefly, after washing the B12-2 cells with PBS and dissociating with cell dissociation reagent (ReLeSR; SCT), the cells were centrifuged at 300 × *g* for 10 min. Thereafter, cells were resuspended in an appropriate volume of neural induction medium supplemented with 10 μM Y-26632 (ROCK inhibitor) at the seeding density of 2×10^5 cells/cm^2 on Matrigel-coated plates. The cells were exposed to NIM for 9 days before splitting them to p2 and maintained in NIM until passage 3 (OCT4 negative/Pax-6 positive). The cells were transferred to neural progenitor medium with 10 μM Y-26632 for the first day after each passage. Further, we examined various proteins involved in DDR in neural progenitor cells.

Differentiation of Neural Progenitor Cells into Astrocytes and Dopaminergic Neurons

Neural progenitor cells were differentiated and allowed to further mature into astrocytes and dopaminergic neurons as per the manufacturer's instructions (Stem Cell Technologies). The cells were characterized using lineage-specific markers (GFAP-astrocytes and TUJ1-dopaminergic neurons).

SUPPLEMENTAL INFORMATION

Supplemental Information includes Supplemental Experimental Procedures and seven figures and can be found with this article online at https://doi.org/10.1016/j.stemcr.2017.10.002.

AUTHOR CONTRIBUTIONS

K.M. and R.K.P. contributed equally. Conception and Design, K.M., W.N.H., C.R.H., N.H., K.K.K, E.B.B., F.M., and T.K.P. Acquisition of Data, K.M., R.K.P., A.T., V.C., S.C., D.K.S., S.H., and N.H. Analysis and Interpretation of Data, K.M., A.Y.K., C.R.H., R.K.P., W.N.H., F.M., and T.K.P. Drafting and Revising the Article, K.M., C.R.H., and T.K.P.

ACKNOWLEDGMENTS

This work was supported by funds from The Houston Methodist Research Institute and grants (CA129537 and GM109768) from the NIH. The authors would like to thank Sendurai A. Mani for providing reagents.

Received: February 23, 2017
Revised: October 4, 2017
Accepted: October 5, 2017
Published: November 2, 2017

REFERENCES

Adams, B.R., Golding, S.E., Rao, R.R., and Valerie, K. (2010). Dynamic dependence on ATR and ATM for double-strand break repair in human embryonic stem cells and neural descendants. PLoS One *5*, e10001.

Anbalagan, S., Bonetti, D., Lucchini, G., and Longhese, M.P. (2011). Rif1 supports the function of the CST complex in yeast telomere capping. PLoS Genet. *7*, e1002024.

Bonetti, D., Clerici, M., Anbalagan, S., Martina, M., Lucchini, G., and Longhese, M.P. (2010). Shelterin-like proteins and Yku inhibit nucleolytic processing of *Saccharomyces cerevisiae* telomeres. PLoS Genet. *6*, e1000966.

Bunting, S.F., Callen, E., Wong, N., Chen, H.T., Polato, F., Gunn, A., Bothmer, A., Feldhahn, N., Fernandez-Capetillo, O., Cao, L., et al. (2010). 53BP1 inhibits homologous recombination in Brca1-deficient cells by blocking resection of DNA breaks. Cell *141*, 243–254.

Chapman, J.R., Barral, P., Vannier, J.B., Borel, V., Steger, M., Tomas-Loba, A., Sartori, A.A., Adams, I.R., Batista, F.D., and Boulton, S.J. (2013). RIF1 is essential for 53BP1-dependent nonhomologous end joining and suppression of DNA double-strand break resection. Mol. Cell *49*, 858–871.

Chlon, T.M., Ruiz-Torres, S., Maag, L., Mayhew, C.N., Wikenheiser-Brokamp, K.A., Davies, S.M., Mehta, P., Myers, K.C., Wells, J.M., and Wells, S.I. (2016). Overcoming pluripotent stem cell dependence on the repair of endogenous DNA damage. Stem Cell Reports *6*, 44–54.

Di Virgilio, M., Callen, E., Yamane, A., Zhang, W., Jankovic, M., Gitlin, A.D., Feldhahn, N., Resch, W., Oliveira, T.Y., Chait, B.T., et al. (2013). Rif1 prevents resection of DNA breaks and promotes immunoglobulin class switching. Science *339*, 711–715.

Escribano-Diaz, C., and Durocher, D. (2013). DNA repair pathway choice–a PTIP of the hat to 53BP1. EMBO Rep. *14*, 665–666.

Escribano-Diaz, C., Orthwein, A., Fradet-Turcotte, A., Xing, M., Young, J.T., Tkac, J., Cook, M.A., Rosebrock, A.P., Munro, M., Canny, M.D., et al. (2013). A cell cycle-dependent regulatory circuit composed of 53BP1-RIF1 and BRCA1-CtIP controls DNA repair pathway choice. Mol. Cell *49*, 872–883.

Feng, L., Fong, K.W., Wang, J., Wang, W., and Chen, J. (2013). RIF1 counteracts BRCA1-mediated end resection during DNA repair. J. Biol. Chem. *288*, 11135–11143.

Fionda, C., Abruzzese, M.P., Zingoni, A., Soriani, A., Ricci, B., Molfetta, R., Paolini, R., Santoni, A., and Cippitelli, M. (2015). Nitric oxide donors increase PVR/CD155 DNAM-1 ligand expression in multiple myeloma cells: role of DNA damage response activation. BMC Cancer *15*, 17.

Gupta, A., Guerin-Peyrou, T.G., Sharma, G.G., Park, C., Agarwal, M., Ganju, R.K., Pandita, S., Choi, K., Sukumar, S., Pandita, R.K., et al. (2008). The mammalian ortholog of *Drosophila* MOF that acetylates histone H4 lysine 16 is essential for embryogenesis and oncogenesis. Mol. Cell Biol. *28*, 397–409.

Gupta, A., Hunt, C.R., Chakraborty, S., Pandita, R.K., Yordy, J., Ramnarain, D.B., Horikoshi, N., and Pandita, T.K. (2014a). Role of 53BP1 in the regulation of DNA double-strand break repair pathway choice. Radiat. Res. *181*, 1–8.

Gupta, A., Hunt, C.R., Hegde, M.L., Chakraborty, S., Udayakumar, D., Horikoshi, N., Singh, M., Ramnarain, D.B., Hittelman, W.N., Namjoshi, S., et al. (2014b). MOF phosphorylation by ATM regulates 53BP1-mediated double-strand break repair pathway choice. Cell Rep. *8*, 177–189.

Henry-Mowatt, J., Jackson, D., Masson, J.Y., Johnson, P.A., Clements, P.M., Benson, F.E., Thompson, L.H., Takeda, S., West, S.C., and Caldecott, K.W. (2003). XRCC3 and Rad51 modulate replication fork progression on damaged vertebrate chromosomes. Mol. Cell *11*, 1109–1117.

Horikoshi, N., Hunt, C.R., and Pandita, T.K. (2016). More complex transcriptional regulation and stress response by MOF. Oncogene *35*, 2681–2683.

Huangfu, D., Osafune, K., Maehr, R., Guo, W., Eijkelenboom, A., Chen, S., Muhlestein, W., and Melton, D.A. (2008). Induction of pluripotent stem cells from primary human fibroblasts with only Oct4 and Sox2. Nat. Biotechnol. *26*, 1269–1275.

Hunt, C.R., Ramnarain, D., Horikoshi, N., Iyengar, P., Pandita, R.K., Shay, J.W., and Pandita, T.K. (2013). Histone modifications and DNA double-strand break repair after exposure to ionizing radiations. Radiat. Res. *179*, 383–392.

Kumar, R., Hunt, C.R., Gupta, A., Nannepaga, S., Pandita, R.K., Shay, J.W., Bachoo, R., Ludwig, T., Burns, D.K., and Pandita, T.K. (2011). Purkinje cell-specific males absent on the first (mMof) gene deletion results in an ataxia-telangiectasia-like neurological phenotype and backward walking in mice. Proc. Natl. Acad. Sci. USA *108*, 3636–3641.

Lan, M.L., Acharya, M.M., Tran, K.K., Bahari-Kashani, J., Patel, N.H., Strnadel, J., Giedzinski, E., and Limoli, C.L. (2012). Characterizing the radioresponse of pluripotent and multipotent human stem cells. PLoS One *7*, e50048.

Li, X., Li, L., Pandey, R., Byun, J.S., Gardner, K., Qin, Z., and Dou, Y. (2012). The histone acetyltransferase MOF is a key regulator of the embryonic stem cell core transcriptional network. Cell Stem Cell *11*, 163–178.

Livak, K.J., and Schmittgen, T.D. (2001). "Analysis of relative gene expression data using real-time quantitative PCR and the 2(-Delta Delta C(T)) method. Methods *25*, 402–408.

Maynard, S., Swistowska, A.M., Lee, J.W., Liu, Y., Liu, S.T., Da Cruz, A.B., Rao, M., de Souza-Pinto, N.C., Zeng, X., and Bohr, V.A. (2008). Human embryonic stem cells have enhanced repair of multiple forms of DNA damage. Stem Cells *26*, 2266–2274.

Mikhed, Y., Gorlach, A., Knaus, U.G., and Daiber, A. (2015). Redox regulation of genome stability by effects on gene expression, epigenetic pathways and DNA damage/repair. Redox Biol. *5*, 275–289.

Momcilovic, O., Choi, S., Varum, S., Bakkenist, C., Schatten, G., and Navara, C. (2009). Ionizing radiation induces ataxia telangiectasia mutated-dependent checkpoint signaling and G(2) but not G(1) cell cycle arrest in pluripotent human embryonic stem cells. Stem Cells *27*, 1822–1835.

Morales, J.C., Xia, Z., Lu, T., Aldrich, M.B., Wang, B., Rosales, C., Kellems, R.E., Hittelman, W.N., Elledge, S.J., and Carpenter, P.B. (2003). Role for the BRCA1 C-terminal repeats (BRCT) protein 53BP1 in maintaining genomic stability. J. Biol. Chem. *278*, 14971–14977.

Mujoo, K., Krumenacker, J.S., and Murad, F. (2011). Nitric oxide-cyclic GMP signaling in stem cell differentiation. Free Radic. Biol. Med. *51*, 2150–2157.

Mujoo, K., Krumenacker, J.S., Wada, Y., and Murad, F. (2006). Differential expression of nitric oxide signaling components in undifferentiated and differentiated human embryonic stem cells. Stem Cells Dev. *15*, 779–787.

Mujoo, K., Sharin, V.G., Bryan, N.S., Krumenacker, J.S., Sloan, C., Parveen, S., Nikonoff, L.E., Kots, A.Y., and Murad, F. (2008). Role of nitric oxide signaling components in differentiation of embryonic stem cells into myocardial cells. Proc. Natl. Acad. Sci. USA *105*, 18924–18929.

Nagane, M., Yasui, H., Sakai, Y., Yamamori, T., Niwa, K., Hattori, Y., Kondo, T., and Inanami, O. (2015). Activation of eNOS in endothelial cells exposed to ionizing radiation involves components of the DNA damage response pathway. Biochem. Biophys. Res. Commun. *456*, 541–546.

Nashun, B., Hill, P.W., and Hajkova, P. (2015). Reprogramming of cell fate: epigenetic memory and the erasure of memories past. EMBO J. *34*, 1296–1308.

Ogiwara, H., Ui, A., Otsuka, A., Satoh, H., Yokomi, I., Nakajima, S., Yasui, A., Yokota, J., and Kohno, T. (2011). Histone acetylation by CBP and p300 at double-strand break sites facilitates SWI/SNF chromatin remodeling and the recruitment of non-homologous end joining factors. Oncogene *30*, 2135–2146.

Oleson, B.J., Broniowska, K.A., Schreiber, K.H., Tarakanova, V.L., and Corbett, J.A. (2014). Nitric oxide induces ataxia telangiectasia mutated (ATM) protein-dependent gammaH2AX protein formation in pancreatic beta cells. J. Biol. Chem. *289*, 11454–11464.

Pacher, P., Beckman, J.S., and Liaudet, L. (2007). Nitric oxide and peroxynitrite in health and disease. Physiol. Rev. *87*, 315–424.

Pandita, R.K., Sharma, G.G., Laszlo, A., Hopkins, K.M., Davey, S., Chakhparonian, M., Gupta, A., Wellinger, R.J., Zhang, J., Powell, S.N., et al. (2006). Mammalian Rad9 plays a role in telomere stability, S- and G2-phase-specific cell survival, and homologous recombinational repair. Mol. Cell Biol. *26*, 1850–1864.

Pandita, T.K. (2013). Histone H4 lysine 16 acetylated isoform synthesis opens new route to biophysical studies. Proteomics *13*, 1546–1547.

Petermann, E., Orta, M.L., Issaeva, N., Schultz, N., and Helleday, T. (2010). Hydroxyurea-stalled replication forks become progressively inactivated and require two different RAD51-mediated pathways for restart and repair. Mol. Cell *37*, 492–502.

Pham-Huy, L.A., He, H., and Pham-Huy, C. (2008). Free radicals, antioxidants in disease and health. Int. J. Biomed. Sci. *4*, 89–96.

Pierce, A.J., Johnson, R.D., Thompson, L.H., and Jasin, M. (1999). XRCC3 promotes homology-directed repair of DNA damage in mammalian cells. Genes Dev. *13*, 2633–2638.

Raschle, M., Knipscheer, P., Enoiu, M., Angelov, T., Sun, J., Griffith, J.D., Ellenberger, T.E., Scharer, O.D., and Walter, J.C. (2008). Mechanism of replication-coupled DNA interstrand crosslink repair. Cell *134*, 969–980.

Rocha, C.R., Lerner, L.K., Okamoto, O.K., Marchetto, M.C., and Menck, C.F. (2013). The role of DNA repair in the pluripotency and differentiation of human stem cells. Mutat. Res. *752*, 25–35.

Schneider, L., Fumagalli, M., and d'Adda di Fagagna, F. (2012). Terminally differentiated astrocytes lack DNA damage response signaling and are radioresistant but retain DNA repair proficiency. Cell Death Differ. *19*, 582–591.

Seita, J., and Weissman, I.L. (2010). Hematopoietic stem cell: self-renewal versus differentiation. Wiley Interdiscip. Rev. Syst. Biol. Med. *2*, 640–653.

Serrano, L., Liang, L., Chang, Y., Deng, L., Maulion, C., Nguyen, S., and Tischfield, J.A. (2011). Homologous recombination conserves DNA sequence integrity throughout the cell cycle in embryonic stem cells. Stem Cells Dev. *20*, 363–374.

Singh, M., Hunt, C.R., Pandita, R.K., Kumar, R., Yang, C.R., Horikoshi, N., Bachoo, R., Serag, S., Story, M.D., Shay, J.W., et al. (2013). Lamin A/C depletion enhances DNA damage-induced stalled replication fork arrest. Mol. Cell. Biol. *33*, 1210–1222.

Tang, J., Cho, N.W., Cui, G., Manion, E.M., Shanbhag, N.M., Botuyan, M.V., Mer, G., and Greenberg, R.A. (2013). Acetylation limits 53BP1 association with damaged chromatin to promote homologous recombination. Nat. Struct. Mol. Biol. *20*, 317–325.

Thomas, T., Dixon, M.P., Kueh, A.J., and Voss, A.K. (2008). Mof (MYST1 or KAT8) is essential for progression of embryonic development past the blastocyst stage and required for normal chromatin architecture. Mol. Cell. Biol. *28*, 5093–5105.

Tran, K.A., Jackson, S.A., Olufs, Z.P., Zaidan, N.Z., Leng, N., Kendziorski, C., Roy, S., and Sridharan, R. (2015). Collaborative rewiring of the pluripotency network by chromatin and signalling modulating pathways. Nat. Commun. *6*, 6188.

Udayakumar, D., Pandita, R.K., Horikoshi, N., Liu, Y., Liu, Q., Wong, K.K., Hunt, C.R., Gray, N.S., Minna, J.D., Pandita, T.K., and Westover, K.D. (2016). Torin2 suppresses ionizing radiation-induced DNA damage repair. Radiat. Res. *185*, 527–538.

van Gent, D.C., Hoeijmakers, J.H., and Kanaar, R. (2001). Chromosomal stability and the DNA double-stranded break connection. Nat. Rev. Genet. *2*, 196–206.

Ward, I.M., Minn, K., van Deursen, J., and Chen, J. (2003). p53 binding protein 53BP1 is required for DNA damage responses and tumor suppression in mice. Mol. Cell. Biol. *23*, 2556–2563.

Weissman, I.L., Anderson, D.J., and Gage, F. (2001). Stem and progenitor cells: origins, phenotypes, lineage commitments, and transdifferentiations. Annu. Rev. Cell Dev. Biol. *17*, 387–403.

Wilson, K.D., Sun, N., Huang, M., Zhang, W.Y., Lee, A.S., Li, Z., Wang, S.X., and Wu, J.C. (2010). Effects of ionizing radiation on self-renewal and pluripotency of human embryonic stem cells. Cancer Res. *70*, 5539–5548.

Zimmermann, M., Lottersberger, F., Buonomo, S.B., Sfeir, A., and de Lange, T. (2013). 53BP1 regulates DSB repair using Rif1 to control 5′ end resection. Science *339*, 700–704.